AIChE

The Dynamics of Single Air Bubbles and Alcohol Drops in Sunflower Oil at Various Temperatures

W. Duangsuwan and U. Tuzun
Dept. of Chemical and Process Engineering, Faculty of Engineering and Physical Sciences, University of Surrey, Guildford, Surrey GU2 7XH, UK

P.A. Sermon
Dept. of Chemistry, Faculty of Health and Medical Sciences, University of Surrey, Guildford, Surrey GU2 7XH, UK

DOI 10.1002/aic.12324
Published online July 13, 2010 in Wiley Online Library (wileyonlinelibrary.com).

Steady rises of a single air bubble, a methanol drop, and an ethanol drop in a vertical glass column of refined sunflower oil at temperatures of 25, 30, 40, and 50°C are investigated experimentally using photography. The Reynolds numbers obtained are 0.07–16, 0.02–13.43, and 0.017–11.18 for the air bubbles, methanol drops, and ethanol drops, respectively. Results for terminal velocity and drag coefficient are compared with the selected existing correlations for bubble and drop motions in immiscible liquids. Correlations by Rodrigue show good agreement for various bubble sizes and system temperatures. Experimental drag coefficients of methanol and ethanol drops show a systematic deviation from the Oliver and Chung and the Darton and Harrison correlations, respectively. Considering the effect of dissolution of alcohol in vegetable oil, which varies with temperature, on the drop dynamics, semiempirical correction factors are applied to the last two correlations to fit the experimental results. © 2010 American Institute of Chemical Engineers *AIChE J,* 57: 897–910, 2011
Keywords: bubble, alcohol drops, sunflower oil, terminal velocity, drag coefficient

Introduction

In an earlier article,[1] the concept of using gas bubble/liquid alcohol compound drops to mix vegetable oil and alcohol in a biodiesel reactor was described as a replacement for a mechanical agitator, and the dynamics of such compound drops in sunflower oil at room temperature were also presented. A gas/alcohol compound drop is a combination of a gas bubble (i.e., air or N_2) and an alcohol liquid drop (i.e., methanol or ethanol). Its dynamics is influenced by the bubble size and the alcohol loading, coupled with the gas/alcohol-, gas/vegetable oil-, and alcohol/vegetable oil interfacial phenomena. With reference to the gas bubble, the engulfing alcohol film can cause its surface to be partly or fully immobile, resulting in the decrease of its terminal velocity. The rise velocity of the alcohol drop is significantly increased by the buoyancy of the gas bubble. As a consequence, information about the dynamics of single gas bubbles and single alcohol drops in vegetable oil is important to improve the understanding about the dynamics of single compound drops. The present experimental investigation aims to observe shapes, rises velocities and drag coefficients of single air bubbles, methanol drops, and ethanol drops rising in sunflower oil at various temperatures. In addition, the results obtained from this study can also provide basic information for other processes in which bubble and vegetable oil are involved, such as refining of vegetable oils using gas bubbles (e.g., Tsiadi et al.[2]).

Correspondence concerning this article should be addressed to W. Duangsuwan at w.duangsuwan@surrey.ac.uk.

Rise of Gas Bubble in Vegetable Oil

Vegetable oil is a Newtonian fluid, which shows a linear relationship between shear stress and shear rate. Boyaci et al.[3] confirmed that vegetable oils (e.g., from cottonseed, olive, hazelnut, corn, sunflower, canola, and soybean) behave as Newtonian fluids at 5–50°C. However, a non-Newtonian behavior (e.g., its viscosity increases with time) due to thermal degradation at high temperature was observed.[4] Experimental study on the motion of gas bubble in vegetable oil has received little attention. Arnold[5] reported the measured terminal velocities of small air bubbles in olive oil at 22°C. Peebles and Garber[6] measured the terminal velocities of single air bubbles in cotton seed oil (at a temperature not stated). Kojima et al.[7] reported the terminal velocities of single air bubbles in castor oil at 31.8°C and Tsiadi et al.[2] studied sizes and shapes of multi-N_2 bubbles in sunflower oil at 18–70°C at and 101 kPa using sintered disc.

A large amount of literature about the rises of gas bubbles in liquids has been published and reviewed for over a century. This has concerned terminal velocity correlations. However, a general correlation for terminal velocity of single gas bubbles in vegetable oil of varying temperatures has not been acknowledged. This literature has been reviewed.[8–15] From these reviews, a few correlations are suitable for gas bubbles in vegetable oils.

In creeping flow, the Stokes equation[16] for a solid sphere can be used to predict the terminal velocity (U_T) of a fully immobile-surface bubble:

$$U_T = \frac{1}{18}\frac{(\rho_o - \rho_i)g d_e^2}{\mu_o} \tag{1}$$

The Hadamard–Rybczynski equation[17,18] for the uncontaminated fluid spheres can also be used to predict the terminal velocity (U_T) of a clean-surface bubble:

$$U_T = \frac{1}{6}\frac{(\rho_o - \rho_i)g d_e^2}{\mu_o}\frac{(\kappa+1)}{(3\kappa+2)} \tag{2}$$

where ρ_o is the density of the continuous liquid [kg/m^3], ρ_i is the density inside the bubble or drop [kg/m^3], g is the gravitational acceleration [kg·m/s^2], d_e is the equivalent diameter of the bubble or drop [m], μ_o is the viscosity of the continuous liquid [Pa s], and $\kappa = \mu_i/\mu_o$ [-] is the viscosity ratio between inside and outside the bubble or drop. The drag coefficient (C_d) in creeping flow for uncontaminated fluid spheres, which corresponds to Eq. 2 is:

$$C_d = \frac{8}{\mathrm{Re}}\left(\frac{3\kappa+2}{\kappa+1}\right) \tag{3}$$

where Reynolds number (Re) is $\rho_o U_T d_e/\mu_o$. Eq. 3 yields the Stokes drag coefficient for a solid sphere when $\kappa = \mu_i/\mu_o = \infty$:

$$C_d = \frac{24}{\mathrm{Re}} \tag{4}$$

and the Stokes drag coefficient for a clean bubble when $\kappa = \mu_i/\mu_o = 0$:

$$C_d = \frac{16}{\mathrm{Re}} \tag{5}$$

For wide ranges of Re and equivalent-sphere bubble diameters (d_e), Jamialahmadi et al.[19] predicted U_T of a single gas bubble:

$$U_T = \frac{U_{T1}U_{T2}}{(U_{T1}^2 + U_{T2}^2)^{1/2}} \tag{6}$$

where U_{T1} is from Eq. 1 for an immobile-surface bubble and Eq. 2 for a fully mobile-surface bubble. U_{T2} is the rise velocity correlation obtained from a wave analogy[20]:

$$U_{T2} = \left[\frac{2\sigma}{d_e(\rho_o - \rho_i)} + \frac{g d_e}{2}\right]^{1/2} \tag{7}$$

where σ is the surface tension of the continuous liquid [N/m].

Rodrigue[12] recommended a correlation for U_T of various bubble sizes by assuming that the liquid is clean (i.e., has no impurities to generate Marangoni stresses) and the gas phase in a gas-liquid system has negligible density and viscosity compared with the liquid phase:

$$U_T = \left(\frac{\sigma\mu_o}{\rho_o^2 d_e^2}\right)^{1/3}\frac{F}{12(1+0.0185F)^{3/4}} \tag{8}$$

where $F = g\left(\rho_o^5 d_e^8/\sigma\mu_o^4\right)^{1/3}$ is the flow number. The drag coefficient corresponding to Eq. 8 was also proposed as being:

$$C_d = \frac{16}{\mathrm{Re}}\left[\begin{array}{l}\left(\frac{1}{2}+32\theta+\frac{1}{2}\sqrt{1+128\theta}\right)^{1/3} \\ \quad +\left(\frac{1}{2}+32\theta-\frac{1}{2}\sqrt{1+128\theta}\right)^{1/3} \\ +\left(0.036\left(\frac{128}{3}\right)^{1/9}\mathrm{Re}^{8/9}M^{1/9}\right)\end{array}\right]^{9/4} \tag{9}$$

where $M = g\mu_o^4/\rho_o\sigma^3$ is the Morton number and $\theta = (0.0185)^3(2/3)^{1/3}\mathrm{Re}^{8/3}M^{1/3}$.

Rise of Alcohol Drop in Vegetable Oil

Dynamics of liquid drop in immiscible liquid-liquid systems is different from that in miscible systems. In immiscible systems the drop sizes during rising (and the system properties) are constant. On the other hand, miscibility affects the surface area, the drag coefficient, and the rise velocity of the drop directly, and alters the thermophysical properties of the surrounding fluid that in turn affects the transfer coefficients of the system.[15] Taylor et al.[21] measured the miscibility of alcohol and vegetable oils and showed that alcohol and vegetable oil are partially miscible. There is more alcohol entering the oil phase than there is oil entering the alcohol phase. This conclusion was confirmed by other observers.[22–27]

Temperature also affects the alcohol-vegetable oil miscibility. Tan et al.[28] indicated that subcritical methanol and oil are immiscible at room temperature, but form a homogenous supercritical solution (239°C and 8.1 MPa). Cerce et al.[29] and Zhou et al.[30] reported that the miscibility of methanol and triglyceride is improved at high temperature. Recently, Liu et al.[31] reported the partial miscibility between Jatropha

oil and methanol, where the mutual solubility increased with temperature and also with the amount of free fatty acids (FFA). When the FFA mass fraction reached 50% in crude Jatropha oil at 60°C, the mixture became completely miscible.

Temperature-dependent partial miscibility of alcohol/vegetable oils leads to an assumption that methanol and ethanol drops will rise in vegetable oil with rates of mass transfer that increase with temperature increases. However, the correlations of the rise velocity and the drag coefficient of liquid drop in immiscible liquid can be used to compare with the experimental results of the drops with mass transfer.

For immiscible liquid drops in Stokes regime (Re $<$ 1), Eqs. 1 and 4 are suitable for an immobile-surface drop, whereas Eqs. 2 and 3 can be used for a clean drop. At Re $>$ 1, some correlations for drag coefficient have been proposed, for example, in Rivkind and Ryskin[32] for 1 $<$ Re $<$ 200, Clift et al.[8] for 4 $<$ Re $<$ 100, and Michaelides[15] for 1 $<$ Re $<$ 20. However, there are four drag coefficient correlations found to be valid for fluid spheres having a wide range of Reynolds numbers, including in creeping flow. The first correlation is from Darton and Harrison,[33] which can be applied for the drops of all Re:

$$C_d = \frac{8(3\kappa+2)}{\mathrm{Re}(\kappa+1)} + \frac{8}{3} \tag{10}$$

Eq. 10 is suitable for bubbles and drops, which change directly from spherical to spherical-cap.[8] The second correlation is from Oliver and Chung,[34] which is suitable for the drops having 0 $<$ Re $<$ 2:

$$C_d = \frac{8}{\mathrm{Re}}\left(\frac{3\kappa+2}{\kappa+1}\right) + 0.4\left(\frac{3\kappa+2}{\kappa+1}\right)^2 \tag{11}$$

The third correlation is from Polyanin and Dilman,[35] which is valid for the drops having 0 $\leq$ Re $\leq$ 100:

$$C_d = \frac{1}{(\kappa+1)}\left(\frac{16}{\mathrm{Re}} + \frac{32}{(\mathrm{Re}+32)}\right) + \frac{\kappa}{(\kappa+1)}\frac{24}{\mathrm{Re}}(1+0.15\mathrm{Re}^{0.687}) \tag{12}$$

Finally, the fourth correlation is from Saboni and Alexandrova,[36] which is suitable for the drops having 0.01 $<$ Re $<$ 400:

$$C_d = \frac{\left[\kappa\left(\frac{24}{\mathrm{Re}} + \frac{4}{\mathrm{Re}^{1/3}}\right) + \frac{14.9}{\mathrm{Re}^{0.78}}\right]\mathrm{Re}^2 + 40\left(\frac{3\kappa+2}{\mathrm{Re}}\right) + 15\kappa + 10}{(1+\kappa)(5+\mathrm{Re}^2)} \tag{13}$$

In case of liquid drops with the presence of mass transfer, the drag coefficient may be predicted from the equation:

$$C_d = \frac{C_{d,0}}{k} \tag{14}$$

where $C_{d,0}$ is the drag coefficient correlation obtained in the absence of mass transfer and k is a correction factor. Eisenklam et al.[37] suggested the following empirical correlation of k for burning fuel drops:

$$k = 1 + B_H \tag{15}$$

where $B_H = c_p\Delta T/\lambda$ is a transfer number for heat transfer, c_p is heat capacity at constant pressure [J/(kg K)], T is temperature [K], λ is latent heat of vaporization [J/kg]. Renksizbulut and Yuen[38] used Eq. 14 for calculating the drag coefficient of an evaporating liquid drop in a high-temperature air flow with the following k:

$$k = (1+B_H)^{0.2} \tag{16}$$

Chuchottaworn and Asano[39] also used Eq. 14 for calculating the drag coefficient of an evaporating or a condensing droplet with Reynolds number, 5 $\leq$ Re $\leq$ 150, and Schmidt number, 0.5 $\leq$ Sc $\leq$ 2.0. They used the following $C_{d,0}$ (Brauer and Sucker[40]) and proposed the following k:

$$C_{d,0} = \frac{24}{\mathrm{Re}} + \frac{3.73}{\mathrm{Re}^{1/2}} - \frac{4.83\times10^{-3}\mathrm{Re}^{1/2}}{1+3\times10^{-6}\mathrm{Re}^{3/2}} + 0.49 \tag{17}$$

$$k = (1+B_M)^{0.19Sc^{-0.74}\cdot(1+B_M)^{-0.29}} \tag{18}$$

where $B_M = (\omega_s-\omega_\infty)/(1-\omega_s)$ is a transfer number for mass transfer, ω_s is the mass fraction of evaporating component at the outer surface of the drop, ω_∞ is the mass fraction of evaporating component in the free stream of the continuous phase.

Experimental Setup

The experimental setup is shown schematically in Figure 1. The 600 mm long circular cross-sectional glass column is divided into three sections, from the top: the 100 mm long and 145 mm I.D. cylindrical top section, the 200 mm long and 35 mm I.D. cylindrical middle section and the 300 mm long conical bottom section. The inside diameters of the top and the bottom ends of the conical section were 16 and 35 mm, respectively. The 65 $\times$ 65 mm square cross-sectional external jacket was made of Plexiglas and filled with pure sunflower oil like in the glass column with the aim of eliminating optical distortion while capturing images of the bubbles or drops with a camera. Sunflower oils in the internal glass column and the external jacket were circulated in the separated closed circuits through the tank of heating water with the flow rates controlled by the variable-speed DC pumps. The temperatures of sunflower oils flowing in the column and the jacket were adjusted to be the same by setting the digital thermostat of the heating tank coupled with controlling the oil flow rates through the variable-speed oil pumps.

PEEKsil capillary tubes from Alltech of I.D. 75 and 150 μm were used to produce the air bubbles of various sizes by connecting them with an air-tight syringe. After circulating sunflower oils in the glass column and the jacket reached the desired setting temperature, the pump for sunflower oil in the glass column was stopped (while the pump for sunflower oil in the jacket was still running to maintain the temperature of the oil inside the column), then the downward flow of the oil in the column stopped. After that the syringe was pressed by hand to let the air flow through the capillary tube, which is vertically submerged in sunflower oil at the bottom end of the column. By this procedure, a stream of bubbles was

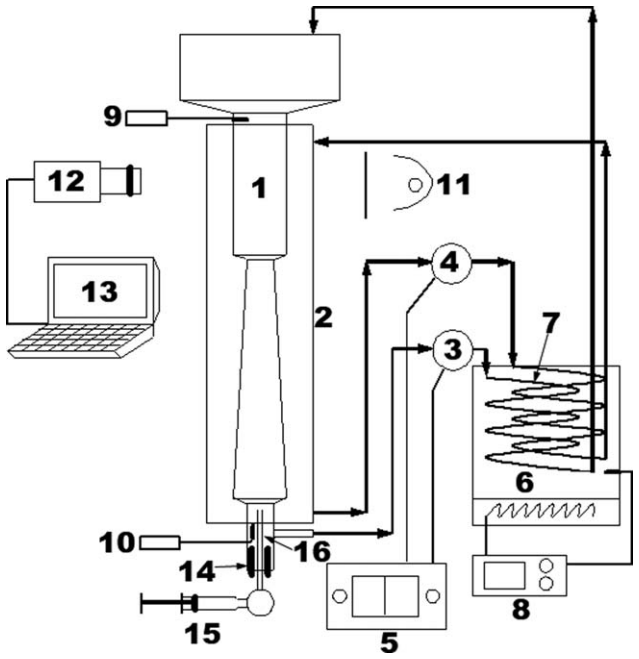

Figure 1. Schematic diagram of experimental setup.

(1) glass column with varying cross-sections filled with sunflower oil; (2) square cross-sectional Plexiglas jacket filled with sunflower oil; (3) and (4) variable speed DC sunflower oil pumps; (5) DC power supply; (6) heating tank filled with water; (7) heating coil-tube of sunflower oil; (8) digital thermostat and temperature sensor; (9) and (10) digital thermometers and temperature sensors; (11) lamp and diffuser; (12) camera; (13) personal computer; (14) rubber stopper; (15) syringe for air or alcohol injections; (16) capillary tube for air injection or syringe needle for alcohol injection.

achieved and the coalescences of some bubbles in the stream and at the capillary tip (during formation and detachment) were observed. After pressing the syringe, the pump was started again and multibubbles were held stationary in the conical section of the column. Decreasing and increasing the pump speed will, respectively, vent the big bubbles upwards and suck the small bubbles downwards out of the conical section. When the only one selected bubble was left, the pump was stopped again, letting the bubble rise freely to the top surface of sunflower oil. For each temperature, the experiments were repeated many times to establish the tendency in the rise velocity of the bubbles for a wide range of bubble sizes.

An Al syringe needle was used instead of the capillary tubes to produce the methanol and the ethanol drops. The I.D. of the needle tip was randomly narrowed by the pliers. The random size multidrops were injected, and only the single drops were selected using the same method described above. It should be noted that the temperatures inside the drops were not measured and may not be the same as the temperature of the sunflower oil continuous phase. However, to minimize the temperature difference between the alcohol drop and the oil, the needle body filled with alcohol was kept in the flow stream of sunflower oil at the desired temperatures for at least 5 min before the syringe's plunger was pressed. In calculation, the temperature inside the alcohol drop was assumed to be the same as the temperature of the oil in the column. PixeLINK PL-A741 monochrome machine vision camera (1 ms shutter speed and 27 frame/s) was used to capture images of bubbles and drops in the middle section of the glass column. Program ImageJ was used for image's pixel analysis. Calibration was via an 8 mm O.D. Al rod.

The properties at various temperatures of sunflower oil (see method of determination in Duangsuwan et al.[1]), methanol, ethanol, and air (Watson[41]; Dean[42,43]; Lide[44]) are shown in Table 1. In the case of alcohol drops rising in sunflower oil, the alcohol dissolution will alter the oil properties, which may have an effect on the rise velocity and the drag coefficient of the drop. Therefore, to reduce this effect, fresh sunflower oil was replaced after each 2 ml of alcohol was introduced into the oil during the experiments. Calculations assumed that the sunflower oil properties at the desired temperatures were not changed.

The nominal shapes of the bubbles and the drops in this work can be roughly classified into three groups (see, Figure 2): (i) sphere with radius a, (ii) oblate spheroid with semimajor axis a and semiminor axis b, and (iii) two-oblate semispheroids with a semimajor axis a and semiminor axes b_1 and b_2. Their equivalent diameters (d_e) were estimated using equations:

$$d_e = 2a \quad \text{(sphere)} \tag{19}$$

$$d_e = [(2b)(2a)^2]^{1/3} \quad \text{(oblatespheroid)} \tag{20}$$

$$d_e = 2a[(b_1 + b_2)/(2a)]^{1/3} \quad \text{(two-oblate semispheroids)} \tag{21}$$

U_T values were calculated using equation:

$$U_T = L/t \tag{22}$$

where $L = ((x_2 - x_1)^2 + (y_2 - y_1)^2)^{1/2}$ is the distance the bubble or the drop rises during the time interval t between two frames ($t = 1/27$ s). The coordinates (x_1,y_1) and (x_2,y_2) , which are obtained during image's pixel analysis, represent the center of mass of the bubble or drop shape in the first and the second frames, respectively.

The balance between the upward buoyancy force of the bubble or drop and the downward drag force and gravitational force yields the equation for calculating the experimental drag coefficients (C_d):

$$C_d = \frac{2gV(\rho_o - \rho_i)}{\rho_o A_p U_T^2} \tag{23}$$

where V and A_p, respectively, are the volume [m^3] and the volume equivalent sphere projected area [m^2] of the bubble or drop.

Results and Discussion

Bubble shape

Because of the limitations of the inside diameter of the middle section glass column (I.D. = 35 mm), which may cause wall effects to the large bubbles and drops, the maximum equivalent diameters (d_e) of the air bubbles and alcohol drops were limited to be ~4.0–6.5 mm. Comparisons between the experimental results and existing correlations (including the correlations with the correction factors) for U_T and C_d of single bubbles and drops rising in liquids of

Table 1. Properties of the System Used

Fluid	Temp. (°C)	Density (kg m^{-3})	Dynamic viscosity (mPa s)	Surface tension (mN m^{-1})	Interfacial tension in contact with sunflower oil (mN m^{-1})
Refined sunflower oil	20	924.7	75.465	32.7	0
	25	921.8	56.863	32.3	0
	30	919.0	43.957	31.8	0
	40	913.3	31.264	31.0	0
	50	907.7	22.648	30.2	0
Methanol	20	792	0.593	22.454	*4.20
	25	787.5	0.551	22.068	*4.15
	30	783	0.514	21.681	*4.07
	40	774	0.449	20.908	*3.98
	50	765	0.395	20.135	*3.88
Ethanol	20	789.45	1.180	22.386	*2.33
	25	785.22	1.074	21.97	*2.32
	30	780.97	0.981	21.554	*2.29
	40	772.50	0.823	20.722	*2.27
	50	764.04	0.694	19.89	*2.24
Air	20	1.204	0.01820	–	32.7
	25	1.184	0.01845	–	32.3
	30	1.165	0.01869	–	31.8
	40	1.127	0.01918	–	31.0
	50	1.093	0.01966	–	30.2

*Estimation was made from equation $\sigma_{AB} = \sigma_A + \sigma_B - 2K(\sigma_A\sigma_B)^{1/2}$ (Girifalco and Good[45]), where σ_A is the surface tension of sunflower oil, σ_B is the surface tension of methanol or ethanol; $K = K_m \times \varphi$, where $K_m = 4(V_A)^{1/3}(V_B)^{1/3}/[(V_A)^{1/3} + (V_B)^{1/3}]^2$, V_A = molar volume of sunflower oil, V_B = molar volume of methanol or ethanol, $\varphi = 1.05$ (obtained by using the soybean oil/methanol interfacial tension from Wu et al.[46]).

infinite extent (i.e., Figures 9, 11, 14–16) confirm that wall effects could be neglected under present conditions.

Air bubbles rising at their terminal velocities in sunflower oil at varying temperatures (see Figure 3) are spherical at $d_e < 2$ mm, but they begin to be oblate ellipsoidal when $d_e = 3$ mm and more ellipsoidal as their volumes and the oil temperatures increase. At 50°C, the bubble shapes begin to distort from ellipsoidal at $d_e \approx 6.5$ mm.

Methanol and ethanol drops shapes

Methanol drops (Figure 4) change from spherical at small diameter to two-oblate semispheroidal at large equivalent diameter, whereas ethanol drops tend to change directly from spherical to dimpled oblate ellipsoidal or oblate ellipsoidal-cap. The ellipsoidal-cap shape of an ethanol drop is obviously observed at 40°C ($d_e = 5$ mm) and 50°C ($d_e = 4$ and 5 mm), whereas at these temperatures and drop sizes, methanol drop remains an ellipsoidal shape.

Figure 5 compares the aspect ratios ($E = (b_1 + b_2)/2a$; see, a, b_1, b_2 in Figure 2) of the bubbles and the alcohol drops. For the air bubbles (Figure 5b), the aspect ratio begins to decrease from 1 at $d_e \approx 1.5$ mm at 25°C (1.7 mm at 50°C). At $E = 0.9$, the bubbles at 25, 30, 40, and 50°C have the values of d_e about 3.4, 3.2, 2.8, and 2.5 mm, respectively, which can be assumed to be spherical. In Figure 5c, the curves clearly show that at the same drop sizes, the ethanol drops change from spherical to ellipsoidal faster than the methanol drops. The methanol drops at 25, 30, 40, and 50°C have $E = 1$ at the values of $d_e \leq 3.0$, 2.6, 2.0, and 1.7 mm, respectively, whereas the ethanol drops at these temperatures show $E = 1$ at the values of $d_e \leq 1.7$, 1.5, 1.0, and 0.7 mm, respectively.

Bubble terminal velocity

Figure 6 compares the terminal velocities of single air bubbles, methanol drops, and ethanol drops rising in sunflower oil at various temperatures. The graph shows that U_T

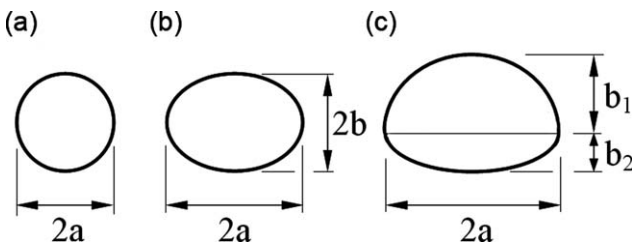

Figure 2. Classification of shapes of bubbles and drops in this work: (a) sphere; (b) oblate spheroid; and (c) two-oblate semispheroids.

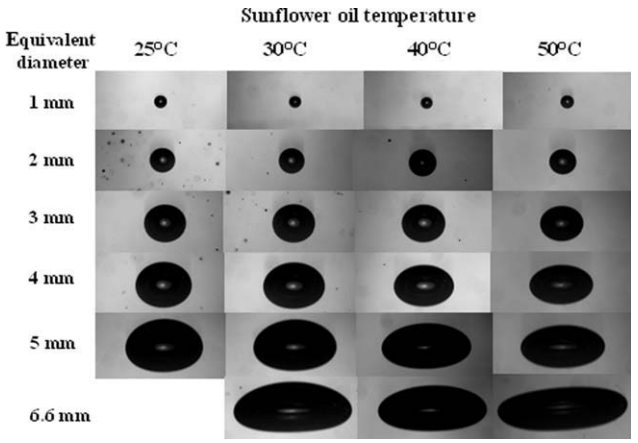

Figure 3. Shapes of bubbles of several equivalent diameters in sunflower oil at varying temperatures.

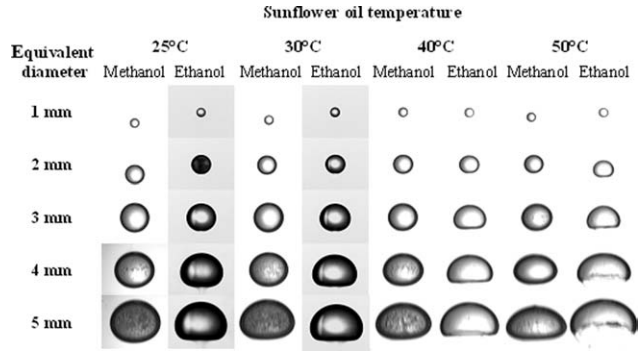

Figure 4. Shapes of methanol and ethanol drops of several equivalent diameters in sunflower oil at varying temperatures.

increases as temperature increases. At 25 and 50°C, the velocities of the bubbles are approximately three and five times that of the alcohol drops.

Figure 7 compares the experimental terminal velocities of the air bubbles with the values predicted by Stokes equation (Eq. 1) and Hadamard–Rybczynski equation (Eq. 2). Figure 7a shows that both equations are not valid for larger bubbles. Figure 7b shows good agreement between experimental results and the Hadamard–Rybczynski equation for the bubbles having diameters smaller than 1.8, 1.5, and 1.2 mm at 25, 30, and 40°C, respectively. At 50°C, although the bubbles of diameter smaller than 1.0 mm are not obtained and shown here, the present results at this temperature show the trend to agree with the Hadamard–Rybczynski equation at bubble diameters smaller than 1.0 mm. For all temperatures, with decreasing diameter below 1.0 mm, the bubble tends to follow Stokes equation rather than Hadamard–Rybczynski equation (see, e.g., at 25°C with $d_e = 0.7$ mm and at 40°C with $d_e = 0.67$ mm). This may be due to the very small amount of surface-active impurities in the oil begins to take effect on the bubble motion (Clift et al.[8]).

Figure 8 shows the comparison between experimental U_T and the values predicted by Eq. 6. The dashed lines, which

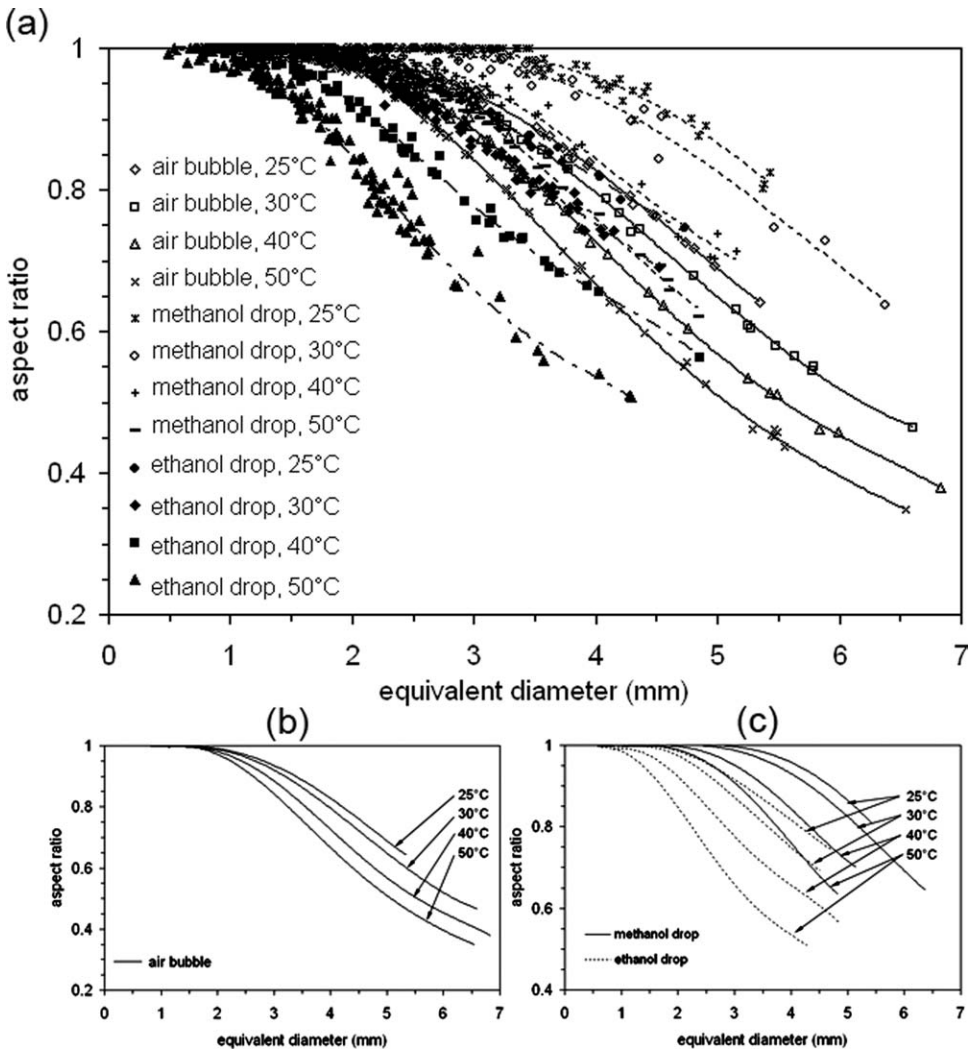

Figure 5. Aspect ratios as functions of equivalent diameters of single air bubbles, methanol drops and ethanol drops rising at terminal velocity in sunflower oil at varying temperatures.

(**a**) Experimental results. (**b**) Trend lines for air bubbles. (**c**) Trend lines for alcohol drops.

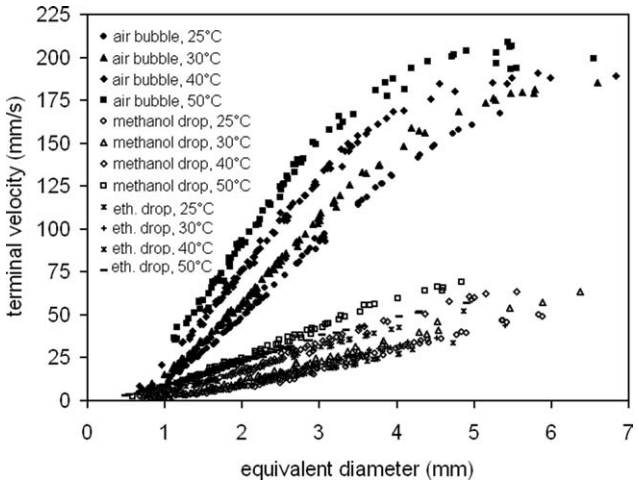

Figure 6. Experimental results showing terminal velocities of single air bubbles, methanol drops and ethanol drops rising in sunflower oil at various temperatures.

represent the predictions for the fully immobile-surface bubbles, are obtained by substituting U_{T1} in Eq. 6 by Eq. 1. Likewise, the solid lines, which represent the prediction for the clean bubbles, are obtained by replacing U_{T1} in Eq. 6with Eq. 2. The solid lines show good prediction for the bubble diameters smaller than 2.2, 1.7, 1.4, and 1.1 mm for the temperatures 25, 30, 40, and 50°C, respectively. Larger than these bubble sizes, the solid lines over-predict for all temperatures except at 50°C that the under-prediction is found at bubble sizes larger than 3.7 mm. The dashed lines show much under-prediction at all temperatures for the bubble diameter up to 5 mm, and are not considered here because of the surfaces of the bubbles not being totally immobile.

Figure 9 compares the experimental results with the values predicted by Rodrigue equation (Eq. 8). Good agreement is obtained at all temperatures for the bubble sizes up to 5 mm. Equation 8 seems to be used as a general correlation for all bubble sizes rising in sunflower oil at all temperatures. The deviation between the predicting values and the experimental values for the bubble diameters higher than 5 mm may be caused by the inaccuracy of measurement of bubble size using image analysis, which is prone to error when analyzing the images of the distorted bubbles.

Methanol and ethanol drops terminal velocities

In cases of methanol and ethanol drops, partial miscibility with sunflower oil may cause the decrease of drop sizes during their rises. Consequently, their rise velocities change all the time. However, if any rise velocity is assumed to be a terminal velocity of the drop at any instantaneous time, Eqs. 1 and 2, which are the lower and upper limits of the terminal velocity of the single drops in immiscible liquids in Stokes flow, may be used for comparison. Figure 10 shows the terminal velocities of methanol and ethanol drops obtained from experiments, Eqs. 1 and 2. It is obviously seen that methanol and ethanol drops follow Eq. 2 rather than Eq. 1 for all temperatures.

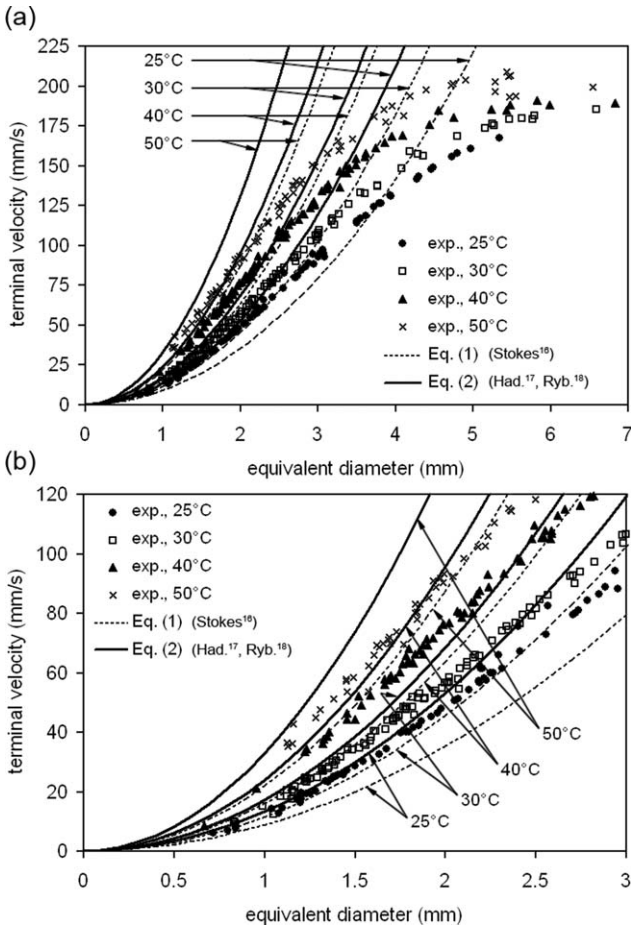

Figure 7. Terminal velocity as a function of equivalent diameter of single air bubbles rising in sunflower oil at varying temperatures, compared to experimental results, Stokes equation (Eq. 1) and Hadamard–Rybczynski equation (Eq. 2).

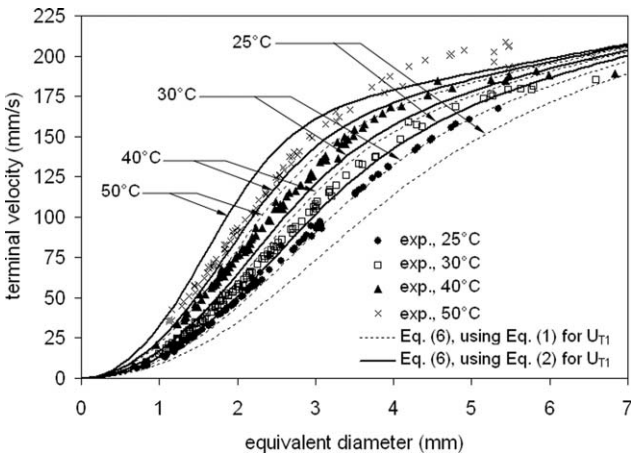

Figure 8. Terminal velocity as a function of equivalent diameter of single air bubbles rising in sunflower oil at varying temperatures, compared to experimental results and Jamialahmadi et al. equation (Eq. 6).

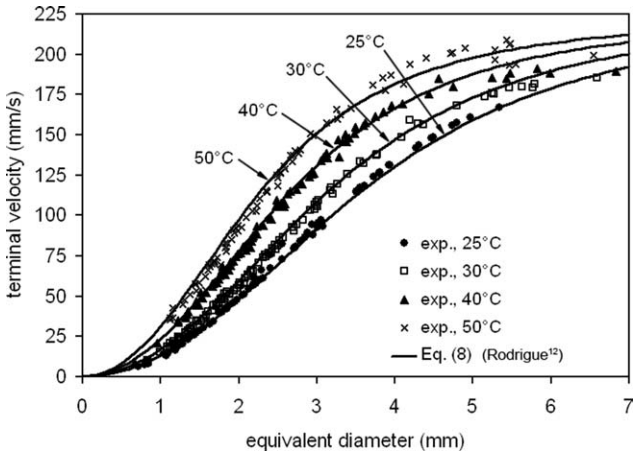

Figure 9. Terminal velocity as a function of equivalent diameter of single air bubbles rising in sunflower oil at varying temperatures, compared to experimental results and Rodrigue equation (Eq. 8).

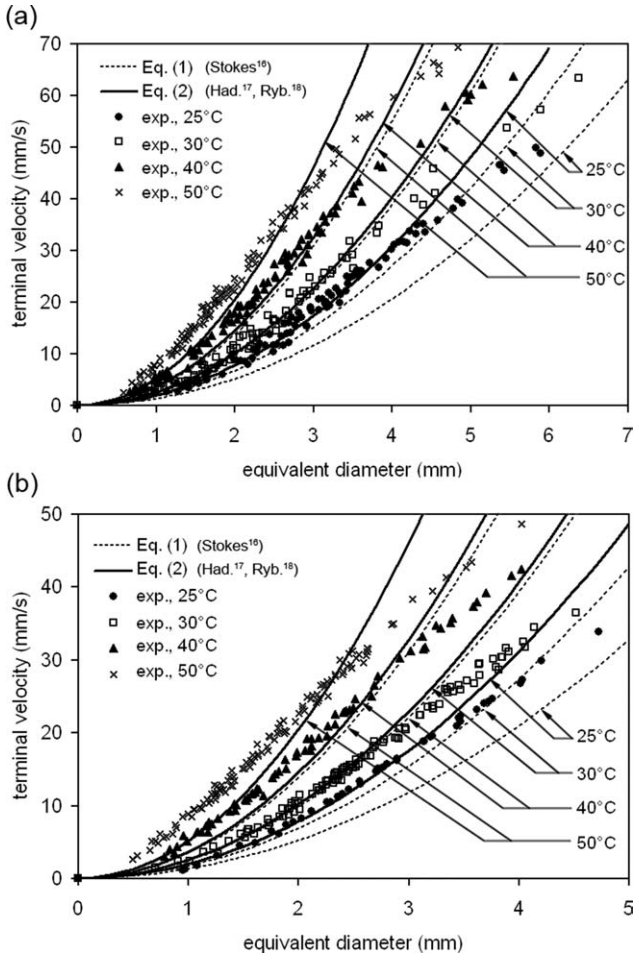

Figure 10. Terminal velocity as a function of equivalent diameter of alcohol drops rising in sunflower oil at varying temperatures, compared to experimental results, Stokes equation (Eq. 1) and Hadamard–Rybczynski equation (Eq. 2).

(**a**) Methanol drops. (**b**) Ethanol drops.

Equation 2 is acceptable for methanol drops having d_e smaller than 4.0 mm (25°C) and 3.5 mm (30°C) and for ethanol drops having d_e smaller than 3.2 (25°C) and 2.8 mm (30°C). These imply that partial miscibility does not have a large effect on the motions of methanol and ethanol drops at low temperatures. With diameter bigger than the above sizes, the correlations for the Stokes flow are not applicable.

Although Eq. 2 presents the upper limit for terminal velocity of a liquid drop in Stokes regime, it is under-estimation for the prediction of the rise velocity of methanol and ethanol drops at 40 and 50°C. This is possibly because the influence of the higher mass transfer rate (compared with the systems at 25 and 30°C) from the alcohol drops to the sunflower oil continuous phase. The deviation of the experimental rise velocities from the values predicted by Eq. 2 at 50°C is larger than that at 40°C and the deviation for ethanol drop is larger than that for methanol drop for both temperatures. This seems to support that the solubility (or miscibility) in sunflower oil for ethanol is higher than that for methanol.

Bubble drag coefficient

Figure 11 shows the comparison of the drag coefficients (C_d) of single air bubbles rising in sunflower oil at varying temperatures, obtained from experiments, Stokes equation (Eq. 4), Hadamard–Rybczynski equation (Eq. 5), and Rodrigue equation (Eq. 9). In logarithmic scale, Eqs. 5 and 9 overlap to each other at $Re < 1$. The experimental C_d follows Eq. 5 (and also Eq. 9) at $0.5 < Re < 1.0$, whereas at $Re \leq 0.5$, it falls between Eqs. 4 and 5. At $Re > 1.0$, where the bubble size increases and the bubble shape is ellipsoidal, the experimental results follow Eq. 9. Therefore, Eq. 9 shows good agreement with experimental results for all Reynolds numbers and temperatures.

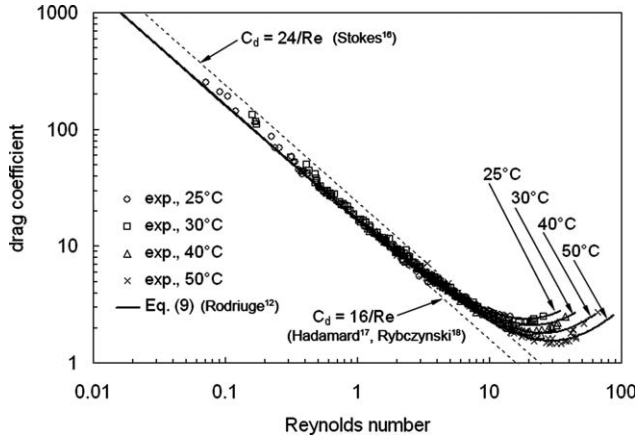

Figure 11. Drag coefficient as a function of Reynolds number of single air bubbles rising in sunflower oil at varying temperatures, compared to experimental results, Rodrigue equation (Eq. 9), Stokes equation (Eq. 4, $C_d = 24/Re$) and Hadamard–Rybczynski equation (Eq. 5, $C_d = 16/Re$).

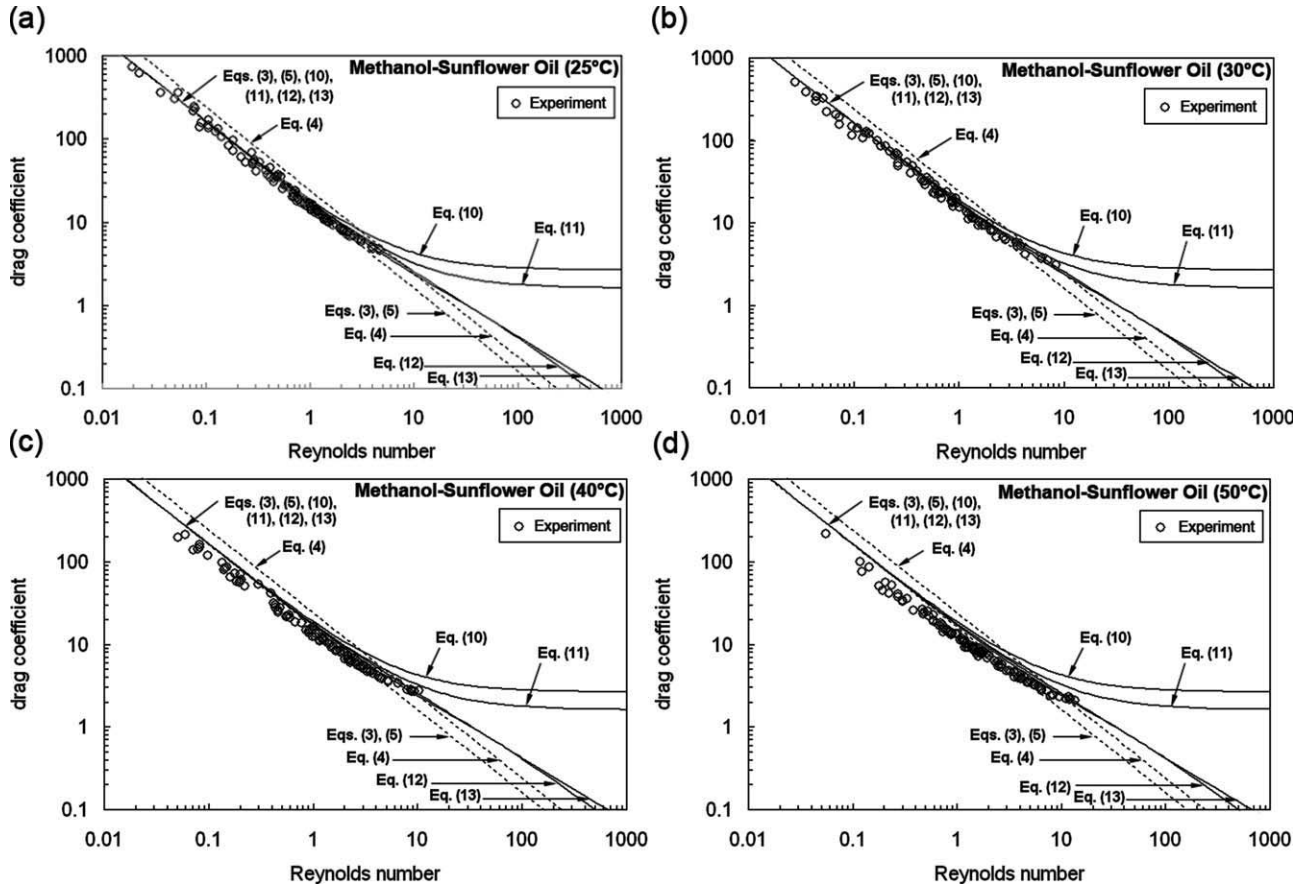

Figure 12. Experimental drag coefficients as functions of Reynolds numbers of methanol drops rising in sunflower oil at varying temperatures compared with the correlations for immiscible liquids.

Methanol and ethanol drops drag coefficients

The plots of C_d as functions of Re of single methanol and ethanol drops rising in sunflower oil at separating temperatures, comparison between experimental results and the correlations for immiscible liquid-liquid systems (i.e., Eqs. 3–5 and Eqs. 10–13), are shown in Figures 12 and 13, respectively. The curves of the predicted C_d obtained from Eqs. 3, 5, 10–13 overlap to each other at $Re < 1$. For all values of Re, the most fitting correlation for methanol drops at 25 and 30°C is the equation of Oliver and Chung (Eq. 11) as shown in Figures 12a, b, whereas for ethanol drops at these temperatures the most fitting correlation is the equation of Darton and Harrison (Eq. 10) as shown in Figures 13a, b. The shapes of ethanol drops in Figure 4 together with the graphs in Figure 13 confirm that Eq. 10 is suitable for the drops that their shapes change directly from spherical to spherical-cap.

At 40 and 50°C and $Re < 3$, Figures 12c, d and Figures 13c, d clearly show that all correlations (for immiscible liquids) shown in the graphs over-predict the experimental C_d. These imply that mass transfer occurs at the drop surface. C_d of methanol drop deviates from Eq. 11, whereas C_d of ethanol drop deviates from Eq. 10.

From above results, Eq. 14 is used for making a correction of C_d. In this case, Eqs. 10 and 11 can be used for $C_{d,0}$ of methanol and ethanol drops, respectively. Unfortunately, the correlations for k for liquid drops moving with mass transfer in gas (Eqs. 15, 16, and 18) cannot be used for the drop moving with mass transfer in liquid, that is, this work. Therefore, using experimental data in hand, the authors can correlate a general semiempirical correlation for k, which can be used for methanol and/or ethanol drops in sunflower oil at varying temperatures. The empirical correlation or the correlation obtained from numerical analysis for k is not shown here. We leave that to those who have much more theoretical skill.

Based on the forms of k (for liquid-gas systems) shown in Eqs. 15, 16, and 18, four forms of k for the present liquid-liquid systems are proposed here:

$$k = a(1 + B_M)^b Sc^d \tag{24}$$

$$k = a(1 + B_M)^b \tag{25}$$

$$k = aSc^d \tag{26}$$

$$k = (1 + B_M)^{a(1+B_M)^b \cdot Sc^d} \tag{27}$$

where $B_M = (X_s - X_\infty)/(1 - X_s)$ is a transfer number for mass transfer, X_s is the mass fraction of dissolving alcohol in sunflower oil at the outer surface of the alcohol drop, X_∞ is the mass fraction of dissolving alcohol in sunflower oil far away

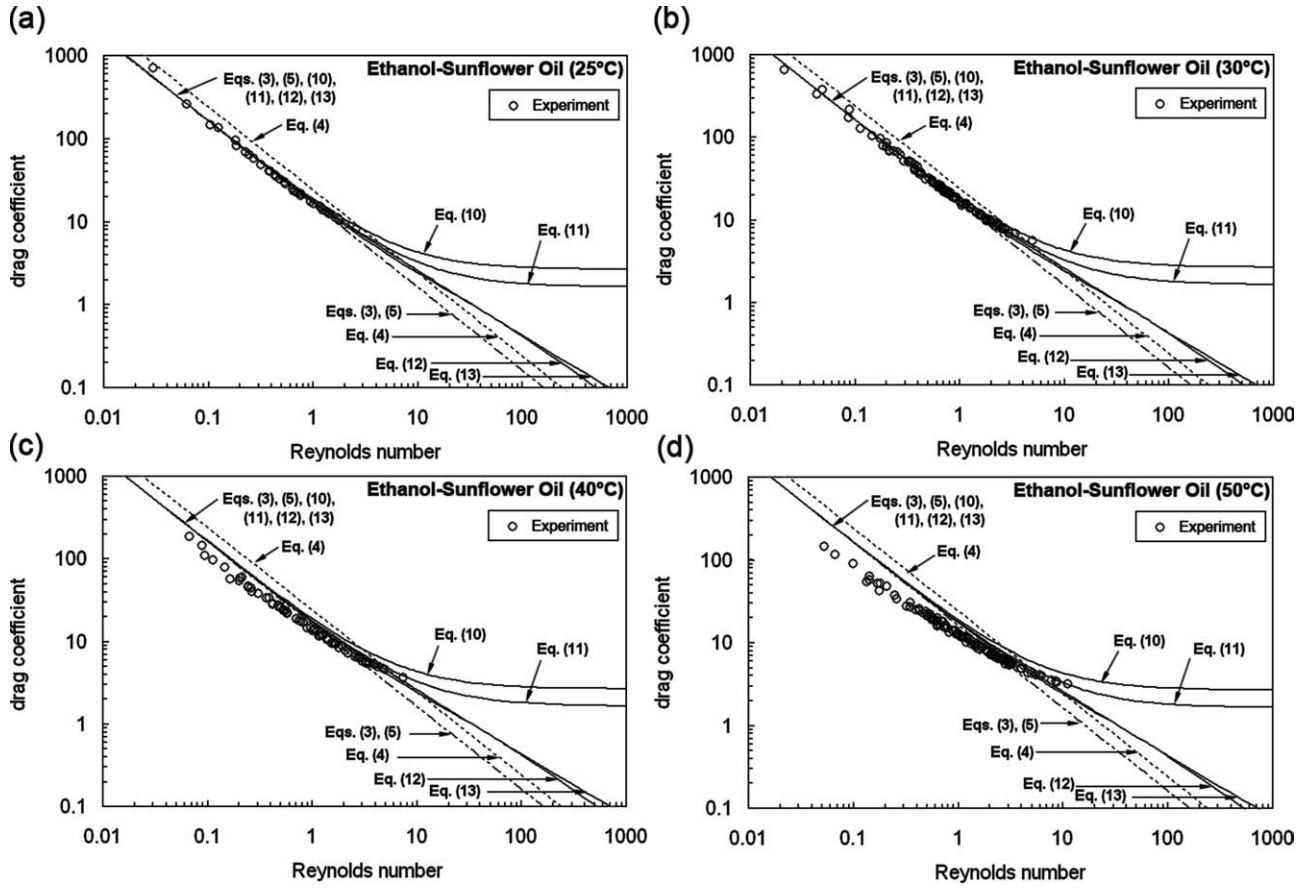

Figure 13. Experimental drag coefficients as functions of Reynolds numbers of ethanol drops rising in sunflower oil at varying temperatures compared with the correlations for immiscible liquids.

from the alcohol drop, $Sc = \mu_o/(\rho_o \cdot D_{AO})$ is the Schmidt number, μ_o is the dynamic viscosity of sunflower oil [Pa s], ρ_o is the density of sunflower oil [kg/m^3], and D_{AO} is the diffusion coefficient of alcohol in sunflower oil [m^2/s].

The experimental values of k are used for determining the values of a, b, and d in Eqs. 24–27. The experimental values of k for methanol and ethanol drops at each temperature are the mean values of k obtained by substituting the experimental drag coefficients as C_d and the predicted drag coefficients (Eq. 11 for methanol drops and Eq. 10 for ethanol drops) as $C_{d,0}$ into Eq. 14. D_{AO} are estimated from Wilke-Chang equation.[47] X_s is assumed to be a mass fraction of alcohol at saturation condition of the alcohol-sunflower oil binary system. Values of X_s at 30 and 40°C for methanol-sunflower oil and ethanol-sunflower oil binary systems are borrowed from Mohsen-Nia and Khodayari.[48] X_s at 25 and 50°C are estimated using the exponential equation obtained from X_s at 30 and 40°C. X_∞ is neglected because of the sunflower oil continuous phase far away from the drop surface is assumed uncontaminated by alcohol. Values of k, X_s, D_{AO}, Sc, and B_M are summarized in Table 2.

Based on Table 2, the correlation constants in Eqs. 24–27 are calculated using multiple regression technique. The calculations are performed separately using the data of each and both type of alcohol drops. The results for a, b, d, and the coefficients of determination (R^2), which represents a goodness of fit, are shown in Table 3. Noting that these values can be changed if one can do measurements, the exact values of X_s and D_{AO}, which may be different from the estimated values shown in Table 2.

Table 2. Values of k, X_s, D_{AO}, Sc, and B_M

Liq.-liq. system	Temperature (°C)	k	X_s	D_{AO} (m^2/s)	Sc	B_M
Methanol-sunflower oil	25	1.129	0.05269	6.82561×10^{-11}	903757.0	0.055619
	30	1.136	0.05785	8.97772×10^{-11}	532778.5	0.061402
	40	1.325	0.06974	1.30390×10^{-10}	262534.8	0.074968
	50	1.449	0.08407	1.85742×10^{-10}	134331.2	0.091791
Ethanol-sunflower oil	25	1.066	0.10454	5.43739×10^{-11}	1134495.0	0.116741
	30	1.107	0.11990	7.15179×10^{-11}	668802.1	0.136234
	40	1.386	0.15773	1.03871×10^{-10}	329562.5	0.187268
	50	1.536	0.20750	1.47965×10^{-10}	168627.3	0.261823

Table 3. Calculated Values of a, b, d, and R^2 for Eqs. 24–27

Equation	Correlation of k	Alcohol	a	b	d	R^2
Eq. 24	$k = a(1+B_M)^b Sc^d$	Methanol	0.5829	8.7230	0.0131	0.965
		Ethanol	8.0647	0.8454	−0.1530	0.961
		Both	8.5737	0.5467	−0.1536	0.942
Eq. 25	$k = a(1+B_M)^b$	Methanol	0.7243	8.0032	–	0.965
		Ethanol	0.7603	3.1410	–	0.944
		Both	1.0833	1.2907	–	0.321
Eq. 26	$k = aSc^d$	Methanol	7.7558	–	−0.1425	0.941
		Ethanol	18.7764	–	−0.2075	0.959
		Both	11.3012	–	−0.1702	0.893
Eq. 27	$k = (1+B_M)^{a(1+B_M)^b Sc^d}$	Methanol	14.7598	11.6724	−0.1875	0.851
		Ethanol	7.08×10^9	−13.7610	−1.5626	0.928
		Both	2.07×10^5	−7.0051	−0.8389	0.829

Neglecting Eq. 27, Table 3 shows that Eqs. 24–26 give values of R^2 between 0.941–0.965 (not different in a goodness of fit) for different types of alcohols. However, Eq. 24 can also provides a single correlation of k (with $R^2 = 0.942$), which can be used for both types of alcohols. For this case, k can be written as:

$$k = 8.5737(1+B_M)^{0.5467} Sc^{-0.1536} \quad \text{(Both alcohol drops)} \tag{28}$$

Alternatively, k can be estimated by using only one variable (i.e., B_M for Eq. 25 or Sc for Eq. 26), but, for each variable, different values of constants a and d are obtained between methanol and ethanol drops. Based on Table 3, k as functions of Sc gives the simplest forms and are written as following:

$$k = 7.7558 Sc^{-0.1425} \quad \text{(Methanol drops)} \tag{29}$$

$$k = 18.7764 Sc^{-0.2075} \quad \text{(Ethanol drops)} \tag{30}$$

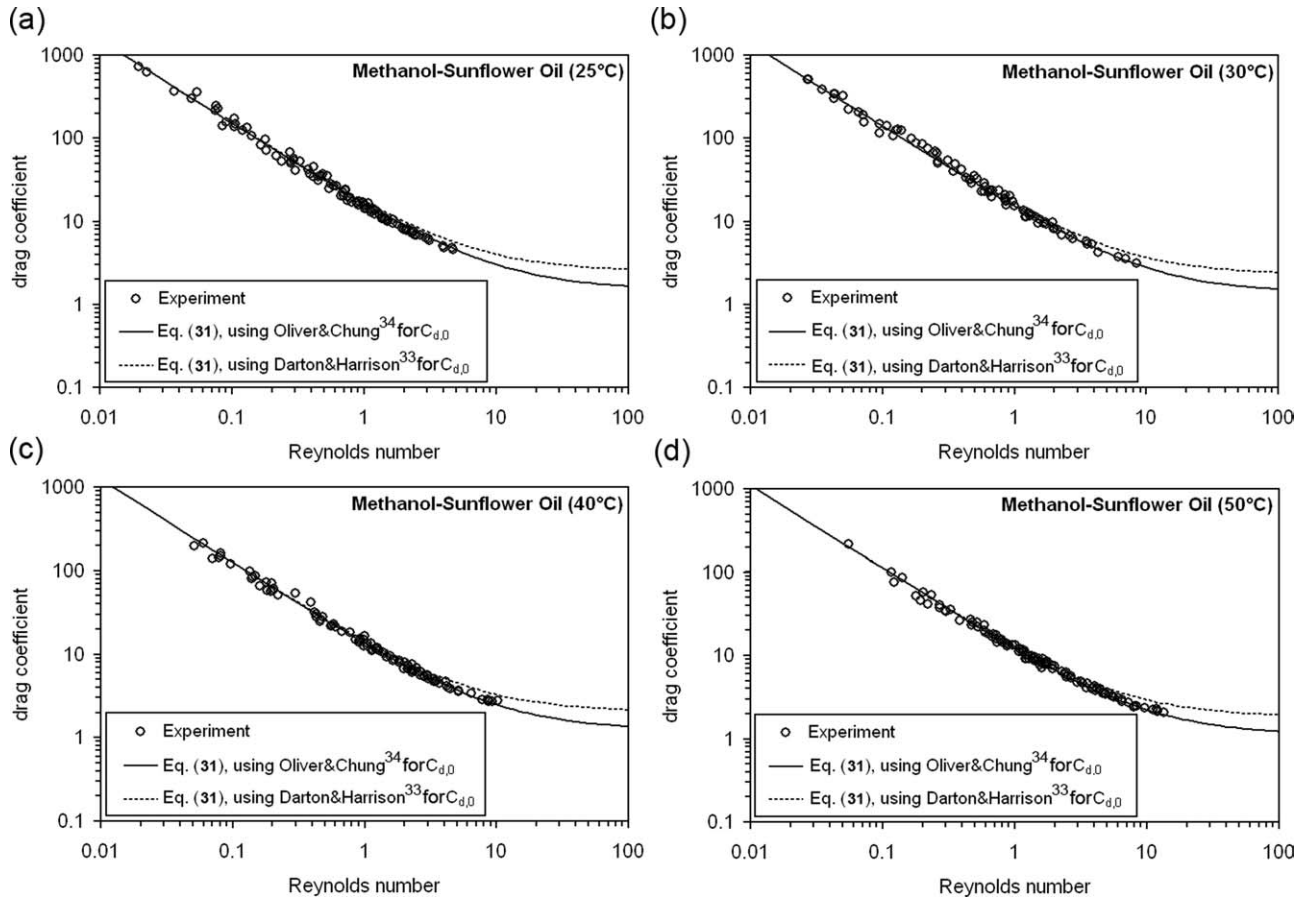

Figure 14. Experimental drag coefficients as functions of Reynolds numbers of methanol drops rising in sunflower oil compared with Eq. 31 (Eqs. 31 and 32 are overlap in logarithmic scale).

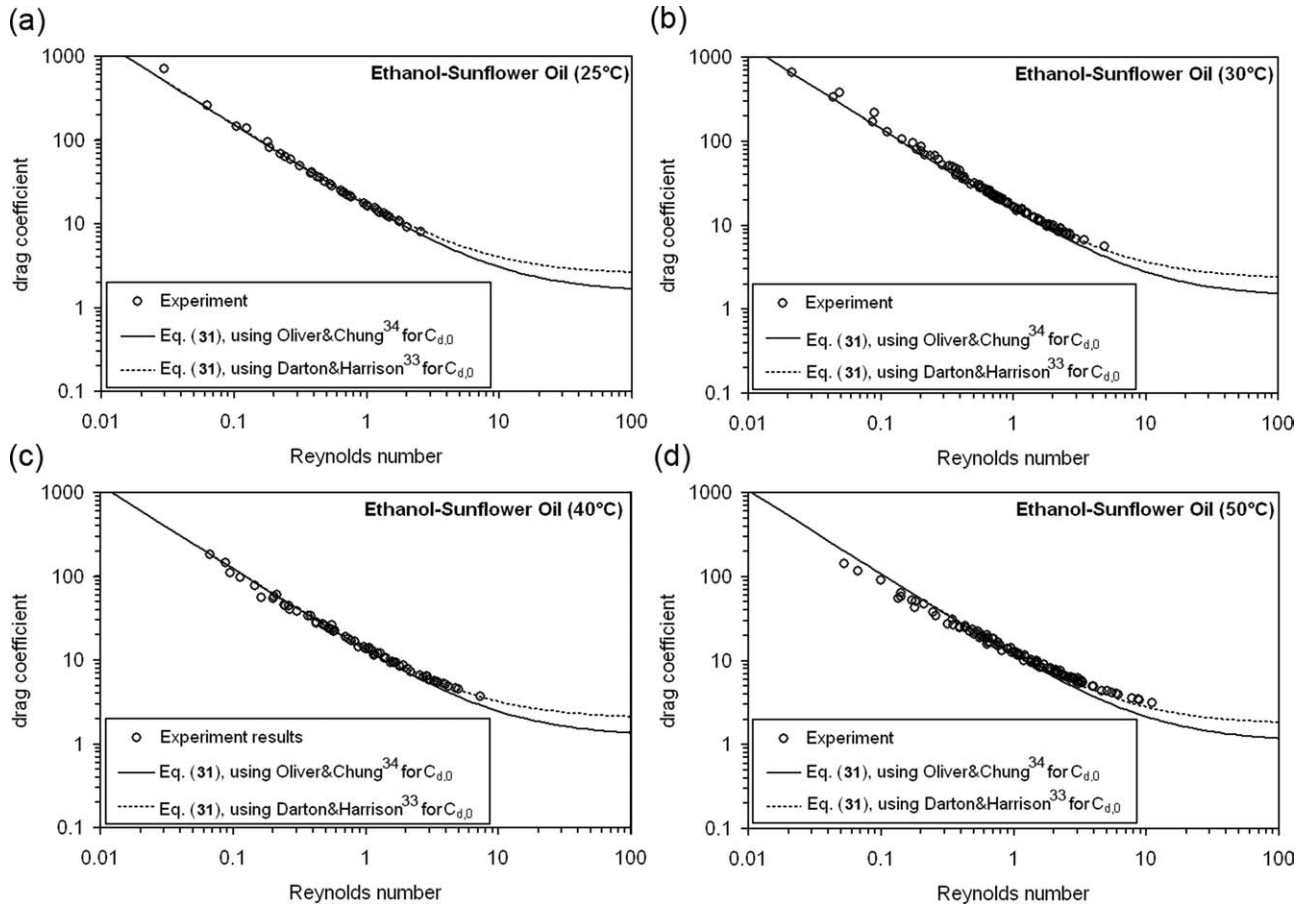

Figure 15. Experimental drag coefficients as functions of Reynolds numbers of ethanol drops rising in sunflower oil compared with Eq. 31 (Eqs. 31 and 33 are overlap in logarithmic scale).

Substituting Eqs. 28–30 into Eq. 14, the semiempirical correlations for C_d of methanol and ethanol drops in sunflower oil are obtained:

$$C_d = \frac{C_{d,0}}{8.5737(1+B_M)^{0.5467}Sc^{-0.1536}} \quad \text{(both alcohol drops)} \tag{31}$$

$$C_d = \frac{C_{d,0}}{7.7558Sc^{-0.1425}} \quad \text{(methanol drops)} \tag{32}$$

$$C_d = \frac{C_{d,0}}{18.7764Sc^{-0.2075}} \quad \text{(ethanol drops)} \tag{33}$$

where $C_{d,0}$ for methanol and ethanol drops are Eqs. 11 and 10, respectively. The relationship of k between the two alcohols is also obtained from Eqs. 29 and 30:

$$\frac{k_{met}}{k_{eth}} = 0.4131\frac{Sc_{eth}^{0.2075}}{Sc_{met}^{0.1425}} \tag{34}$$

where the subscripts "met" and "eth" refer to methanol and ethanol, respectively.

Figures 14 and 15 compare C_d predicted by Eq. 31 with C_d from experiments for methanol and ethanol drops, respectively. Good agreement is observed. Eq. 32 and Eq. 33 are not shown in these figures due to plotting Eqs. 31 and 32 or Eqs. 31 and 33 in the same graph makes the curves overlap in logarithmic scale.

Equation 14 also yields a correlation of U_T for methanol drops:

$$0.4\left[\frac{3\kappa+2}{\kappa+1}\right]^2 U_T^2 + \frac{8\mu_o}{\rho_o d_e}\left[\frac{3\kappa+2}{\kappa+1}\right]U_T - \frac{4}{3}\frac{gd_e(\rho_o-\rho_i)k}{\rho_o} = 0 \tag{35}$$

and for ethanol drops:

$$\frac{8}{3}U_T^2 + \frac{8\mu_o}{\rho_o d_e}\left[\frac{3\kappa+2}{\kappa+1}\right]U_T - \frac{4}{3}\frac{gd_e(\rho_o-\rho_i)k}{\rho_o} = 0 \tag{36}$$

where k could be obtained from Eq. 28 for both methanol and ethanol drops if B_M and Sc of each alcohol are known, or from Eq. 29 or 30 for methanol and ethanol drops, respectively, if Sc of each alcohol is known. Figure 16 compares U_T from experiments with U_T predicted from Eqs. 35 and 36. The experimental data show good agreement with these correlations.

Conclusions

Experimental results showing shapes, terminal rise velocities, and drag coefficients of single air bubbles, methanol drops, and ethanol drops rising in sunflower oil at various temperatures have been obtained. The fitting correlations for

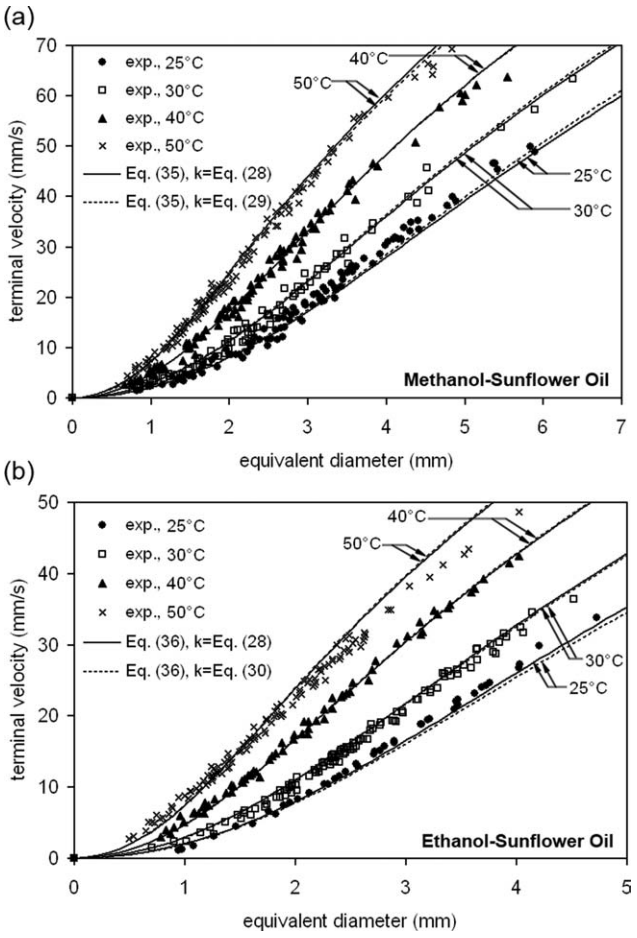

Figure 16. Experimental terminal rise velocities of methanol and ethanol drops compared with the proposed correlations.

(**a**) Methanol drops with Eq. 35. (**b**) Ethanol drops with Eq. 36.

terminal velocity and drag coefficient have been found from literature. The Hadamard–Rybczynski correlations agree well with the terminal velocities and the drag coefficients of the small bubbles at all temperatures and of the small alcohol drops at 25 and 30°C. The Rodrige correlation fits well with the terminal velocities of the bubbles of various bubble sizes and system temperatures. For all sizes of alcohol drops at room temperature, the drag coefficient correlations of Oliver and Chung (1987) and Darton and Harrison (1974) show good predictions for methanol drops and ethanol drops, respectively. However, because of the dissolution of alcohols from alcohol drops in sunflower oil significantly influencing the drop motions at higher temperatures, the semiempirical correction equations for drag coefficient of the drops are made and can be used for all temperatures (25–50°C). Consequently, the correlations for terminal velocity of the drops are obtained. The correction equations for drag coefficient and terminal velocity agree well with experimental results.

Acknowledgments

Funding for this study by the Government of the Kingdom of Thailand, under the Thai-UK Collaborative Research Network scheme, is gratefully acknowledged.

Literature Cited

1. Duangsuwan W, Tüzün U, Sermon PA. Configurations and dynamics of single air/alcohol gas-liquid compound drops in vegetable oil. *Chem Eng Sci*. 2009;64:3147–3158.
2. Tsiadi AV, Stavrides E, Handa-Corrigan A. Nitrogen bubble dynamics in sunflower oil at atmospheric pressure. *Food Bioprod Process*. 1999;77:281–286.
3. Boyaci IH, Tekin A, Cizmeci M, Javidipour I. Viscosity estimation of vegetable oils based on their fatty acid composition. *J Food Lipids*. 2002;9:175–183.
4. Rubalya Valantina S, Neelameagam P. A Study of rheological behavior and oxidative stability of rice bran and corn oil using FTIR spectra. *IJPAP*. 2008;4:77–86.
5. Arnold HD. Limitations imposed by slip and inertia terms upon Stokes's law for the motion of spheres through liquids. *Philos Mag*. 1911;22:755–775.
6. Peebles FN, Garber HJ. Studies on the motion of gas bubbles in liquids. *Chem Eng Prog*. 1953;49:88–97.
7. Kojima E, Akehata T, Shirai T. Rising velocity and shape of single air bubbles in highly viscous liquid. *J Chem Eng Jpn*. 1968;1:45–50.
8. Clift R, Grace JR, Weber ME. *Bubbles, Drops, and Particles*. New York: Academic Press, 1978.
9. Perry RH, Green DW. *Perry's Chemical Engineers' Handbook*, *6th ed*. New York: McGraw-Hill, 1984.
10. Grace JR, Waigeri T. Properties and characteristics of drops and bubbles. In: *Encyclopedia of Fluid Mechanics* (Vol 3, N.P. Cheremisinoff, Ed., *Chap 3*). Houston: Gulf Publishing, 1986:43–57.
11. Happel J, Brenner H. *Low Reynolds Number Hydrodynamics*, 5th ed. Dordrecht, The Netherlands: Kluwer, 1991.
12. Rodrigue D. Generalized correlation for bubble motion. *AIChE J*. 2001:47;39–44.
13. Polyanin AD, Kutepov AM, Vyazmin AV, Kazenin DA. *Hydrodynamics Mass and Heat Transfer in Chemical Engineering*. Boca Raton: CRC Press, 2002.
14. Kulkarni AA, Joshi JB. Bubble formation and bubble rise velocity in gas-liquid systems: a review. *Ind Eng Chem Res*. 2005:44;5873–5931.
15. Michaelides EE. *Particles, Bubbles and Drops: Their Motion, Heat and Mass Transfer*. Singapore: World Scientific Publishing, 2006.
16. Stokes GG. On the effect of the internal friction of fluids on the motion of pendulum. *Trans Cambridge Philos Soc*. 1851:9;8–106.
17. Hadamard JS. Mouvement permanent lent d'une sphe're liquide et visqueuse dans un liquide visqueux. *C R Acad Sci*. 1911;152: 1735–1738.
18. Rybczynski W. On the translatory motion of a fluid sphere in a viscous medium. *Bull Acad Sci Cracow Ser A*. 1911;40–46.
19. Jamialahmadi M, Branch C, Müller-Steinhagen H. Terminal bubble rise velocity in liquids. *Trans Inst Chem Eng*. 1994:72;119–121.
20. Mendelson HD. The prediction of bubble terminal velocities from wave theory. *AIChE J*. 1967:13;250–253.
21. Taylor TI, Larson L, Johnson W. Miscibility of alcohol and oils. *Ind Eng Chem*. 1936:28;616–618.
22. Noureddini H, Zhu D. Kinetics of transesterification of soybean oil. *J Am Oil Chem Soc*. 1997;74:1457–1463.
23. Ma F, Hanna MA. Biodiesel production: a review. *Bioresour Technol*. 1999:70;1–15.
24. Chiu CW, Goff MJ, Suppes GJ. Distribution of methanol and catalysts between biodiesel and glycerin phases. *AIChE J*. 2005;51: 1274–1278.
25. Liu X, Piao X, Wang Y, Zhu S. Liquid-liquid equilibrium for systems of (fatty acid ethyl esters + ethanol + soybean oil and fatty acid ethyl esters + ethanol + glycerol). *J Chem Eng Data*. 2008;53: 359–362.
26. Dunn RO, Bagby MO. Low-temperature phase behaviour of vegetable oil/co-solvent blends as alternative diesel fuel. *J Am Oil Chem Soc*. 2000;77:1315–1323.
27. Chen JW, Wu WT. Regeneration of immobilized Candida Antarctica lipase for transesterification. *J Biosci Bioeng*. 2003;95:466–469.
28. Tan KT, Lee KT, Mohamed AR. Production of FAME by palm oil transesterification via supercritical methanol technology. *Biomass Bioenergy*. 2009:33;1096–1099.
29. Cerce T, Peter S, Weidner E. Biodiesel-transesterification of biological oils with liquid catalysts: thermodynamic properties of oil-methanol-amine mixtures. *Ind Eng Chem Res*. 2005;44:9535–9541.

30. Zhou H, Lu H, Liang B. Solubility of multicomponent systems in the biodiesel production by transesterification of Jatropha curcas L. oil with methanol. *J Chem Eng Data*. 2006;51:1130–1135.
31. Liu Y, Lu H, Liu C, Liang B. Solubility measurement for the reaction systems in pre-esterification of high acid value Jatropha curcas L. Oil. *J Chem Eng Data*. 2009;54:1421–1425.
32. Rivkind VY, Ryskin GM. Flow structure in motion of a spherical drop in a fluid medium at intermediate Reynolds numbers. *Fluid Dyn*. 1976;11:5–12.
33. Darton RC, Harrison D. The rise of single gas bubbles in liquid fluidized beds. *Trans Inst Chem Eng*. 1974;52:301–306.
34. Oliver DLR, Chung JNC. Flow about a fluid sphere at low to moderate Reynolds numbers. *J Fluid Mech*. 1987;177:1–18.
35. Polyanin AD, Dilman VV. *Methods of Modelling Equations and Analogies in Chemical Engineering*. Boca Raton: CRC Press, 1994.
36. Saboni A, Alexandrova S. Numerical study of drag on a fluid sphere. *AIChE J*. 2002:48;2992–2994.
37. Eisenklam P, Arunachalam SA, Weston JA. Evaporation rates and drag resistance of burning drops. Proceedings of the 11th International Symposium on Combustion. The Combustion Institute, Pittsburgh, PA, 1967;715–728.
38. Renksizbulut M, Yuen MC. Experimental study of droplet evaporation in high temperature air stream. *J Heat Transf*. 1983;105: 384–388.
39. Chuchottaworn P, Asano K. Calculation of drag coefficients of an evaporating or a condensing droplet. *J Chem Eng Jpn*. 1985;18:91–94.
40. Brauer H, Sucker D. Flow about plates, cylinders and spheres. *Int Chem Eng*. 1978;18:367–374.
41. Watson JTR. *Viscosity of Gases in Metric Units*. Edinburgh, Her Majesty's Stationery Office: Crown copyright, 1972.
42. Dean JA. *Lange's Handbook of Chemistry*, *11th ed*. New York: McGraw-Hill, 1973.
43. Dean JA. *Lange's Handbook of Chemistry*, *13th ed*. New York: McGraw-Hill, 1985.
44. Lide DR. *Handbook of Chemistry and Physics*, *81st ed*. London: CRC, 2000.
45. Girifalco LA, Good RJ. A theory for the estimation of surface and interfacial energies. I. Derivation and application to interfacial tension. *J Phy Chem*. 1957;61:904–909.
46. Wu P, Yang Y, Colucci JA, Grulke EA. Effect of ultrasonication on droplet size in biodiesel mixtures. *J Am Oil Chem Soc*. 2007;84: 877–884.
47. Poling BE, Prausnitz JM, O'Connel JP. *The Properties of Gases and Liquids*, 5th ed. New York: McGraw-Hill, 2004.
48. Mohsen-Nia M, Khodayari A. De-acidification of sunflower oil by solvent extraction: (Liquid + liquid) equilibrium data at T = (303.15 and 313.15) K. *J Chem Thermodynamics*. 2008;40: 1325–1329.

Manuscript received Oct. 9, 2009, revision received Mar. 4, 2010, and final revision received Jun. 4, 2010.